Comparison of various models for strain-softening

Gilles Pijaudier-Cabot*, Zdeněk P. Bažant and Mazen Tabbara
Department of Civil Engineering, Center for Concrete and Geomaterials, Northwestern University, Tech-2410, Evanston, IL 60208, USA
(Received February 1988)

ABSTRACT

This paper presents a comparison of various models for strain-softening due to damage such as cracking or void growth, as proposed recently in the literature. Continuum-based models expressed in terms of softening stress–strain relations, and fracture-type models expressed in terms of softening stress–displacement relations are distinguished. From one-dimensional wave propagation calculations, it is shown that strain-localization into regions of finite size cannot be achieved. The previously well-documented spurious convergence is obtained with continuum models, while stress–displacement relations cannot model well smeared-crack situations. Continuum models may, however, be used in general if a localization limiter is implemented. Gradient-type localization limiters appear to be rather complicated; they require solving higher-order differential equations of equilibrium with additional bourdary conditions. Non-local localization limiters, especially the non-local continuum with local strain, in which only the energy dissipating variables are non-local, is found to be very effective, and also seems to be physically realistic. This formulation can correctly model the transition between homogeneous damage states and situations in which damage localizes into small regions that can be viewed as cracks. The size effect observed in the experimental and numerical response of specimens in tension or compression is shown to be a consequence of this progressive transition from continuum-type to fracture-type formulations.

INTRODUCTION

Numerous models have recently been proposed to describe the post-peak strain-softening response of concrete, rocks, metals with void growth, and other materials. In this intensely debated subject, two fundamentally different macroscopic approaches may be distinguished: (1) softening stress–strain relations, the traditional approach for concrete, and (2) softening stress–displacement relations, an approach coopted from ductile fracture of metals.

The softening stress–strain relations, which describe smeared cracking, characterize the damage due to cracking in a continuum sense. We may mention for example the endochronic or fracturing theories[1], the continuum damage mechanics[2,3], the void growth models such as Gurson's[4,5], the smeared-crack approach[6,7], and the viscoplastic formulations of Needleman and Sandler[8,9]. For continuum models, questions such as the uniqueness and stability of the solution when the tangential stiffness matrix becomes negative definite must be addressed. As documented in previous studies[10,11], spurious localization occurs in numerical calculations, giving rise, in the limit of vanishing mesh size, to physically unacceptable solutions without any dissipation of energy.

The softening stress–displacement relations were introduced by Hillerborg[12], and applied by Ingraffea[13] and Willam *et al.*[14,15]. This approach is obviously more focused on the modelling of distinct, line cracks. However, it has not yet been shown that this approach could be applied to distributed cracking situations, for example to uniaxial loading of confined specimens[3,16] or more importantly to situations where failure involves the interaction of many cracks.

The purpose of this paper is to discuss the properties of each approach. We will show that the material and structural descriptions constitute limiting cases where the physical damage that produces softening is either distributed, in the statistical sense, or localized into infinitesimal zones. To this end, we will analyse longitudinal wave propagation in one dimension, applying several recently proposed models, and study especially the energy dissipated due to damage along with its density distribution over the structure and evolution in time.

In both types of models, the conditions of finiteness of the total energy and the energy density at failure cannot be met simultaneously. The softening response of the material with a finite (non-zero size) of the strain-localization zone cannot be described properly even for the rate-dependent models for which the dynamic problem is mathematically well posed. With regard to similar phenomena in fluid mechanics, it may be helpful to consider strain-softening as a transitory response caused by change in the type of the governing partial differential equations of motion from hyperbolic to elliptic, similar to that encountered in hypersonic flow or in fluid–structure interaction[17].

Inspired by recent solutions such as the Taylor–Galerkin method[18] or upwinding techniques[19,20], constitutive laws or continuum models with higher-order spatial derivatives have been proposed[21–23]. Transposed to the mechanics of solids, the physical significance of these models, especially the additional boundary and interface conditions in terms of high order derivatives, may appear questionable. In most cases it may be convenient to consider these formulations as non-local models in which the quantity that is averaged is expanded in Taylor series[24]. This latter type of approach appears to be simple in its implementation and provides satisfactory results in terms of the energy distributed at failure.

WAVE PROPAGATION IN STRAIN-SOFTENING MATERIALS

To compare strain-localization behaviour of various models, we choose to analyse the propagation of longitudinal waves in a one-dimensional medium, i.e. a bar. The one-dimensional setting has the advantage that closed-form solutions can be derived for some strain-softening situations[25]. The differential equation of

* Present address: Research Associate, Rensselaer Polytechnic Institute, Troy, NY 12180, USA.

0264–4401/88/020141–10$2.00

motion has the form $\rho u_{,tt} = \sigma_{,x}$ where the subscripts following a comma denote partial derivatives; u = displacement, σ = uniaxial stress, and ρ = mass per unit length. If a constitutive law of the form $\sigma = F(\varepsilon)$ is assumed, where $\varepsilon = u_{,x}$ = uniaxial strain, the equation of motion becomes:

$$u_{,tt} = v^2 u_{,xx} \tag{1}$$

in which $v = [F'(\varepsilon)/\rho]^{1/2}$ = wave velocity. This equation is hyperbolic if v is real, that is, if the tangential modulus $F'(\varepsilon)$ of the material is positive. As pointed out in numerous studies, $F'(\varepsilon)$ is negative in strain-softening situations, causing the differential equation of motion (1) to change its type from hyperbolic to elliptic. This change, called Hadamard instability[17], indicates that strain-softening should not propagate.

The bar is initially stress-free and at rest at time $t = 0$. As the boundary conditions, we assume that for $t \geq 0$ the end points of the bar, $x = -L$ and $x = L$, are forced to move outward at constant velocities $-c$ and c. If the material is elastic, with elastic modulus E, this produces two step waves of constant strain, $\varepsilon_0 = c/v$. At time $t_m = L/c$, at which the waves meet at the centre of the bar ($x = 0$), the strain is doubled ($\varepsilon = 2\varepsilon_0$) if $2\varepsilon_0$ remains within the elastic range. On the other hand, if c is such that $0.5 f_t' < c < f_t'$ where f_t' = strength limit after which strain softening begins, one obtains strain-softening at the middle of the bar, $x = 0$, at time $t = t_m$.

The solution for $t > t_m$ has been given by Bažant and Belytschko[25] for the case of a local medium. This solution shows that unloading elastic step waves which reduce the strain at $x \neq 0$ from ε_0 to 0 emanate from point $x = 0$ while the strain at $x = 0$ becomes instantly infinite. The bar splits at $x = 0$, a finite gap forms and its width grows at constant velocity. The strain-softening zone does not propagate but remains confined to a single point ($x = 0$). Consequently, the splitting of the bar in the middle is indicated to occur at zero energy dissipation. This feature is not physically realistic.

For real materials, the dissipation of energy due to failure must be finite. Moreover, in view of some experimental observations of damage locations by the acoustic emission technique[26] in certain materials such as concrete, it is unrealistic to consider strain-softening (due to damage, e.g. microcracking) to remain limited to a region of zero thickness. Therefore, we require a material model for which the dissipation in the strain-softening zone is finite. We also desire a model for which the strain-softening zone thickness is finite, before a localized failure is observed.

For each material model discussed, we study the evolution of the strain and stress profiles after the medium enters the strain-softening regime (for $t > t_m$). We focus attention on the dissipation of energy due to softening, W_s (see *Figure 1c*; the bar cross-section is 1),

$$W_s = \int_{-L}^{L} \bar{W}_s(x)\,\mathrm{d}x = \int_{-L}^{L}\int_{0}^{t} \bar{W}_{s,t}\,\mathrm{d}x\,\mathrm{d}t \tag{2}$$

where $\bar{W}_s$ = energy dissipation density and $\bar{W}_{s,t}$ = rate of $\bar{W}_s$. We assume the material to be elastic, i.e. $F'(\varepsilon)$ = constant up to the peak stress. Then, if the peak-stress has not yet been reached at point x, we have $\bar{W}_s = 0$, and after that

$$\bar{W}_s = \frac{1}{2}\left[\mathrm{d}\left(\frac{\sigma^2}{E_u}\right) - \sigma\,\mathrm{d}\varepsilon\right] \tag{3}$$

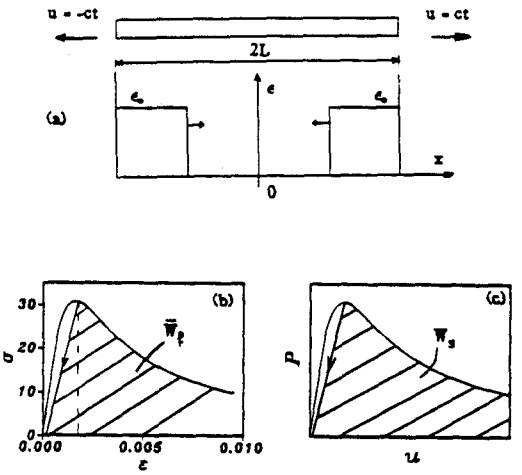

Figure 1 (a) Wave propagation in a bar; (b) definition of the specific softening energy; and (c) softening energy

in which E_u is the unloading modulus. The specific energy at failure $\bar{W}_f$ at point x is defined by $\bar{W}_f = \int_0^\infty \bar{W}_{s,t}\,\mathrm{d}t$. It is represented by the cross-hatched area under the σ–ε curve in *Figure 1b*.

We solve the problem numerically by finite elements, using an explicit time-integration technique. We consider different element subdivisions with an increasing number N of elements of constant length and look primarily at the convergence of the energy dissipation W_s. On physical grounds, W_s should tend for $N \to \infty$ to a finite value, which corresponds to the underlying continuum solution. The strain and stress profiles further clarify how the energy dissipating process is distributed over the bar.

STRUCTURAL APPROACH

First, we consider the formulations, developed for concrete, in which the strain-softening behaviour is modelled by a stress–displacement law. Proposed by Hillerborg and others[12–15,27], this type of material model is inspired by ductile fracture mechanics. It takes the view that strain-softening in two-dimensional structures is concentrated into such a small part of the structure that it may be considered as a crack (fictitious crack). Consequently the softening response of the structure is not described in terms of strains, which are singular, but in terms of the relative displacements across the softening zone (a line). In a certain sense, this type of model is aimed at a global description of the fracture process zone rather than a detailed, local description of the damage distribution.

Corroborated by experiments, a similar model called the 'composite fracture model', was recently proposed by Willam *et al.*[15]. In this model, strain-softening in tension is described by a stress–displacement law, such that the energy release rate which must be equal to the fracture energy, G_f, of the material is kept constant independently of the size of the specimen, i.e. $G_f = \int_0^\infty \sigma\,\mathrm{d}u = \text{const}$.

The finite element model may be summarized, for the case of loading, by the following relations:

$$\begin{aligned} &\text{If } \varepsilon < \varepsilon_p \text{ then } \sigma = E\varepsilon \\ &\text{If } \varepsilon \geq \varepsilon_p \text{ then } \sigma = E_d u_f - \sigma_p, \quad u_f = u - \varepsilon_p L_e \end{aligned} \tag{5}$$

where E = Young's modulus of the material, L_e = length

of the bar or finite element, $\varepsilon_p=\sigma_p/E$=strain at peak stress σ_p; u_f=post-peak relative displacement of the bar or element of length L_e due to fracturing; and E_d=softening modulus, which is deduced from the fracture energy as follows:

$$E_d=\frac{\sigma_p^2}{2G_f} \tag{6}$$

The softening modulus of the homogeneous equivalent continuum, E_f, is not constant but is computed from E_d depending on the size L_e of the specimen or finite element $E_f=E_dL_e$. *Figure 2a* presents the stress *versus* mean strain diagrams for bars of various lengths. For unloading and reloading, $\Delta\sigma=E\Delta\varepsilon$.

With this type of model a constant energy is dissipated when localization occurs. A good convergence in terms of energy is obtained from the finite element solution of the wave propagation problem, despite the fact that localization in zones of non-zero length cannot be achieved. As pointed out by Willam *et al.*[15], this may be due to a lack of spatial resolution of the model, which cannot capture very localized tensile cracking and its inherent strain discontinuity.

Similar to Bažant and Belytschko's solution for the continuum model[25], we may obtain an analytical solution of wave propagation for the composite fracture model. We consider two convergent waves of constant strain in a bar of length $2L$ (*Figure 1a*). The boundary conditions are:

$$\begin{aligned}&\text{For } x=-L: \quad u=-ct\\ &\text{For } x=L: \quad u=ct\end{aligned} \quad \text{with} \quad \frac{\varepsilon_p}{2}<\frac{c}{v}<\frac{\varepsilon_p}{2} \tag{7}$$

where v=wave velocity and $\varepsilon_p=\sigma_p/E$=strain at peak stress. Before the two waves meet ($t<t_m$), the solution of the equations of motion is:

$$u(x,t)=-c\left\langle t-\frac{x+L}{v}\right\rangle+c\left\langle t+\frac{x-L}{v}\right\rangle \tag{8}$$

where the symbol $\langle\ \rangle$ is defined by $\langle x\rangle=(x+|x|)/2$.

For $t>t_m$, where $t_m=L/v$, the two waves have already met at $x=0$. Similar to Reference 25, we seek the solution of the equation of motion in a small portion of the bar of length $2s$, centred at $x=0$, where softening is observed. Wave propagation is governed by an elliptic partial differential equation of motion:

$$\alpha^2u_{,xx}+u_{,tt}=0, \quad \text{with} \quad \alpha^2=\frac{E_d}{2s\rho} \tag{9}$$

At the interface the stress jump $\Delta\sigma$ is related to the strain jump $\Delta\varepsilon$ by (10)[25],

$$\Delta\sigma=\rho\Delta\varepsilon v^2 \tag{10}$$

If s is finite the strain-softening modulus in segment $2s$ is $E_f=2sE_d$ across the interface $x=s$, the jump in stress is negative (i.e. the stress is less in the softening segment than outside) while the jump in strain is positive. Therefore v^2 is negative, and so s remains infinitesimal. If $s\to 0$, the softening modulus becomes zero and the response in the segment of length $2s$ is elastic perfectly plastic. Therefore $\Delta\sigma=0$ and $v^2=0$ for $s\to 0$, i.e., the partial differential equation of motion becomes parabolic.

The solution of (9) for $t\geqslant t_m$ and $x>0$ can be obtained[25] for the case of infinitesimal s as follows:

$$u(x,t)=c\left\langle t+\frac{x-L}{v}\right\rangle+c\left\langle t-\frac{x+L}{v}\right\rangle-\frac{v\sigma_p}{E}\left\langle t-\frac{x+L}{v}\right\rangle \tag{11}$$

For $x<0$, the solution is symmetric. The strain field for $x>0$ is:

$$\varepsilon=\frac{c}{v}\left[H\left(t+\frac{x-L}{v}\right)+H\left(t-\frac{x+L}{v}\right)\left(1-\frac{\sigma_p}{E}\right)\right]+4\langle vt-L\rangle\delta(x) \tag{12}$$

H is the Heaviside function and δ is the Dirac delta function. Softening is confined at the point $x=0$. For

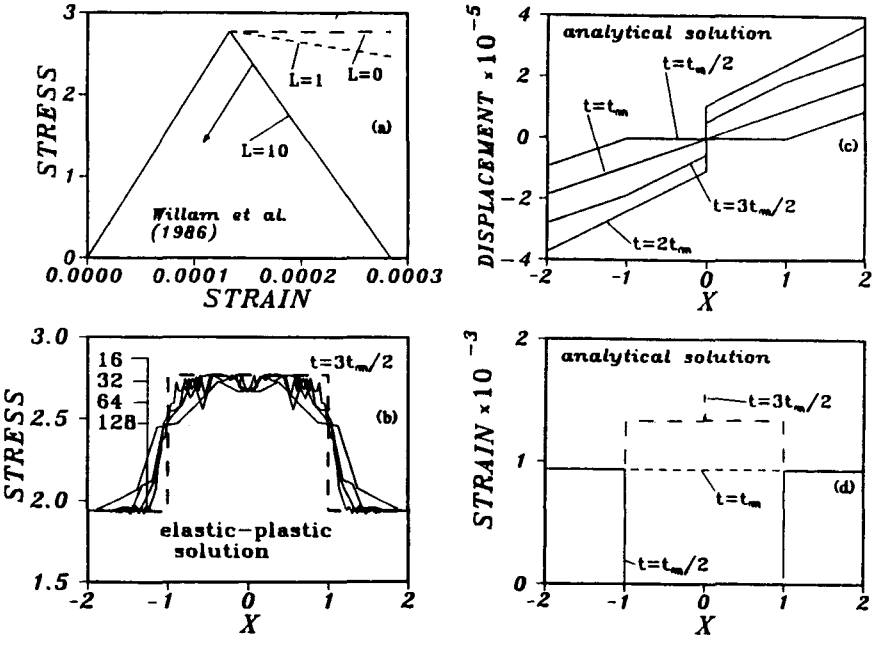

Figure 2 (a) Composite fracture model; (b) convergence of the stress profiles when the mesh is refined; (c, d) analytical displacement and strain profiles

$t_m < t < 2t_m$, the fracture energy that is dissipated may be expressed as a function of the displacement jump:

$$W_s = \sigma_p \delta u = 4\sigma_p c\left(t - \frac{L}{v}\right) \tag{13}$$

At any given time $t > t_m$, W_s is non-zero (this would not be true for a continuum).

Figures 2c and *2d* show the displacement and strain profiles obtained analytically. The material parameters are the same as used by Willam *et al.*[14]: $E = 20{,}748$ MPa, $E_f = 1841$ MPa, $\sigma_p = 2.77$ MPa, $\rho = 0.25 \times 10^{-5}$ kg/mm^3 and $c = 8.5$. After the two waves have met, a step strain wave of magnitude ε_p (strain at peak-stress) is reflected from the middle of the bar. The response is similar to an elastic perfectly plastic bar in which a yield front propagates toward the bar ends.

The finite element approximation of the solution is compared in *Figure 2b* to the analytical stress profile. Despite numerical oscillations, a good convergence is obtained when the mesh is refined and, in the limit of a large number of finite elements, agreement with the analytical solution is achieved. The strain, however, localizes into a zone of zero-size (a point). Good as it is at describing the final failure mode of the bar, this material model is incapable of describing distributed cracking situations, which have been detected experimentally[26] for studies preceding the final strain-localization.

TIME INDEPENDENT CONTINUUM MODEL

Spurious convergence of the fracturing and continuum damage models developed for concrete and geomaterials has already been demonstrated[1,10,11,21,28] and an analytical solution for wave propagation has been derived for general constitutive laws of continua[25]. Because of Hadamard instability and other difficulties, it was suggested by some authors[29] that strain-softening may not be an admissible property of a continuum.

Mathematically equivalent models in which softening resulted from micromechanics consideration of the material degradation have also been proposed. Expanding the model of Gurson[4], Needleman and Tvergaard[5] developed a material model for the ductile failure of metals where softening is the result of a strain (or stress)-induced void growth in a hardening plastic matrix. Simplified to one dimension and small strains, the constitutive law may be expressed as follows. The behaviour of the matrix is:

$$\begin{aligned} &\text{If } \sigma < \sigma_y \quad \text{then} \quad \sigma_m = E\varepsilon_m \\ &\text{If } \sigma \geq \sigma_y \quad \text{then} \quad \varepsilon_m = \frac{\sigma_y}{E}\left(\frac{\sigma}{\sigma_y}\right)^n \end{aligned} \tag{14}$$

Subscript m refers to the matrix; σ_y = yield stress of the matrix, E = Young's modulus, and n = material constant. The elastic strain rate $\dot{\varepsilon}^e$ satisfies Hooke's law. The total strain rate is $\dot{\varepsilon} = \dot{\varepsilon}^e + \dot{\varepsilon}^p$, where $\dot{\varepsilon}^p$ = plastic strain rate, which may be deduced from the work equivalence condition:

$$\sigma \dot{\varepsilon}_p = (1-f)\sigma_m \dot{\varepsilon}_m^p \tag{15}$$

where f is the void ratio of the material. A plastic potential, Φ_p, is used, and its expression is derived from micromechanics considerations[4]:

$$\Phi_p = \frac{\sigma^2}{\sigma_m^2} + 2f^* \cosh\left(\frac{\sigma}{2\sigma_m}\right) - \{1 - (q_1 f^*)^2\} \tag{16}$$

where q_1 is a material parameter, and f^* is a function of the void ratio,

$$f^* = \begin{cases} f & \text{for } f < f_c \\ f_c + \dfrac{f_u^* - f_c}{f_F - f_c}(f - f_c) & \text{for } f \geq f_c \end{cases} \tag{17}$$

and f_u^*, f_c, f_F are material parameters. In the example solved here, the law of void nucleation and void growth is assumed in the form:

$$\dot{f} = (1-f)\dot{\varepsilon}^p + A\left(\frac{EE_t}{E - E_t}\right)\dot{\varepsilon}_m^p \tag{18}$$

in which E_t = tangential modulus of the matrix, and A = statistical parameter governing the void nucleation.

Using the parameter values given in Reference 5, except that $\varepsilon_N = 0.1$, one obtains the stress–strain curve in *Figure 3a*. Comparison with the hardening curve of the matrix shows that softening is due to the presence of voids. Obviously the specific energy at failure of this material $\bar{W}_f$, defined in *Figure 1*, is finite; $\bar{W}_f = 0.2517$.

The overall response of this model is very close to continuum damage mechanics although the unloading stiffness is preserved rather than degraded. This is because it is assumed that the voids remain continuously distributed (smeared). Despite its physical basis which may certainly appear more realistic than the damage theory, it is found that this model possesses all the spurious properties inherent to strain-softening. *Figures 3b* and *3c* show the result of the wave propagation analysis ($\rho = 0.243 \times 10^{-7}$, $c = 0.7$, time-step $\Delta t = 0.2 \times 10^{-7}$). For $t = 1.5t_m$ (88 time-steps), the void ratio and strain profiles exhibit a strong localization near the boundaries $x = -L$, and $x = L$ ($L = 0.5$), comparable to the wave-trapping phenomenon[30]. To observe softening, the boundary conditions are chosen such that the incoming waves are in the hardening range. Consequently the wave velocity is dramatically decreased (because of the high ductility) and plastic strain accumulates at the boundaries. Eventually, before strain-softening is produced by the waves propagating toward the middle of the bar, strain localization occurs at the bar ends. *Figure 3c* shows that the void ratio starts to grow at $x = 0, x = -2$ and $x = 2$. Finally, it becomes particularly concentrated at $x = -2$ and $x = 2$, indicating that softening localizes in these two points. Therefore the energy dissipation due to softening W_s (*Figure 6*) becomes zero as the finite element solution converges toward the continuum solution. Localization into zones of zero volume implies that the strain states located beyond the peak-stress point contribute nothing to the total energy dissipated by the structure. The solutions are the same as if softening was replaced by a sharp, discontinuous drop of the stress to zero once the peak-stress is reached.

RATE-DEPENDENT CONTINUUM MODEL

Propagation of the strain-softening zone cannot be obtained in a continuum because the equations of motion are elliptic. As pointed out[9,17,21], the Cauchy problem becomes for such conditions ill-posed and cannot be solved by the Galerkin method. The Cauchy problem is well-posed if the equations of motion remain hyperbolic. Recently it has been shown that this change of type in the governing partial differential equation from hyperbolic to elliptic can be prevented by introducing

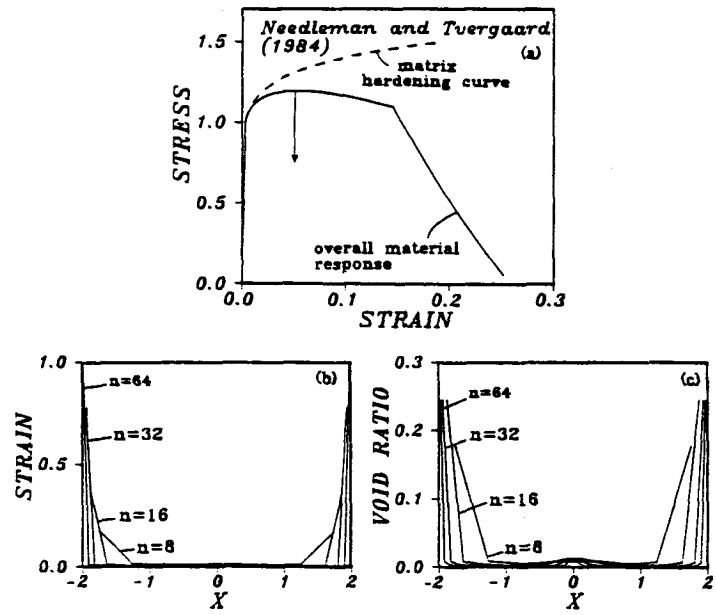

Figure 3 (a) Ductile failure model; convergence of the strain (b) and void (c) profiles with mesh refinement

rate-dependent models. Discussed by Needleman[8] in the context of shear localization and by Lasry and Belytschko[21] for spherical waves, a simple rate-dependent model may be summarized as follows. The stress rate $\dot{\sigma}$ is given by:

$$\dot{\sigma} = E(\dot{\varepsilon} - \dot{\varepsilon}^p) \tag{19}$$

where $\dot{\varepsilon}$ and $\dot{\varepsilon}^p$ are the strain and plastic strain rates respectively, and E is the Young's modulus. Viscoplasticity is introduced into the evolution of the plastic strain:

$$\dot{\varepsilon}^p = \dot{a}(\sigma/g)^{1/m} \tag{20}$$

$\dot{a}$ and m are material parameters and g is a function of the effective plastic strain $\bar{\varepsilon} = \int |\dot{\varepsilon}_p| \, dt$:

$$\begin{aligned} &\text{If } \varepsilon_p < \varepsilon_m \quad \text{then} \quad \dot{g} = H_1|\dot{\bar{\varepsilon}}| \\ &\text{If } \varepsilon_p \geq \varepsilon_m \quad \text{then} \quad \dot{g} = H_2|\dot{\bar{\varepsilon}}|, \text{and } g(0) = \sigma_0 \end{aligned} \tag{21}$$

We choose the material parameter values to be the same as in Reference 8, except that $\varepsilon_m = 0.2\sigma_0/E$ since we want to limit the hardening portion of the response. We take $E = 500$, $m = 0.02$, and for finite element analysis we chose $\rho = 0.413 \times 10^{-7}$, $c = 148.5$, and $\Delta t = 0.2 \times 10^{-6}$ to 8×10^{-9}, depending on the finite element size.

For loading at a constant strain rate the time integration gives the stress–strain curve depicted in *Figure 4a*. The numerical results on wave propagation are presented in *Figure 4b* and are also compared to the analytical solution for an elastic material of the same modulus E. Despite some computational problems already reported[8,21], reasonably convergent results are obtained. It should be noted that this finite element solution is almost identical to the elastic solution except at $x = 0$ (*Figures 4b* and *4c*). Localization occurs at $x = 0$, although the strain is finite. In fact viscosity prevents the strains from becoming infinite and the failure is observed only if a sufficient number of time steps are carried out.

However, this basic improvement compared to the rate-independent model does not appear to be a complete answer to strain-softening problems. *Figure 4d* shows the distribution of the energy $\bar{W}_s$ dissipated by softening in each finite element, for meshes of 64 and 128 elements. As strain localization becomes sharper and sharper, the energy dissipation becomes more and more confined to the middle elements. The total energy dissipated (i.e., the area under the curve in *Figure 4d*) decreases as the softening zone size tends to zero. So the same argument as explained for the rate-independent models becomes applicable. In the limit, failure is obtained without any dissipation due to softening, and a finite size of the localization zone is not possible, even though the wave propagation equations are well-posed.

LOCALIZATION LIMITERS

Localization into a zero-size zone is obtained for both the continuum and fracture mechanics approaches. In the continuum approach, cracking is assumed to be uniformly distributed and if it localizes spurious results are encountered, while the fracture mechanics approach may be applied only after the strain-localization takes place. To combine both descriptions, the so-called localization limiters were recently developed[11] in various forms. Basically two types of limiters may be distinguished. Inspired from fluid mechanics[17–20], the first type consists in the use of higher-order spatial derivative in the constitutive law. As pointed out by Donea[17], this aspect may sometimes be related to rate-dependent formulations. The second type of localization limiters uses non-local averaging procedures to smooth out the strain distributions.

Higher-order spatial derivatives may be introduced either into the elastic potential for hyperelastic materials[16] or simply into the constitutive law[21,22,31,32]. Schreyer and Chen developed such a model in which plastic strains are controlled by the strain gradient[22]. For

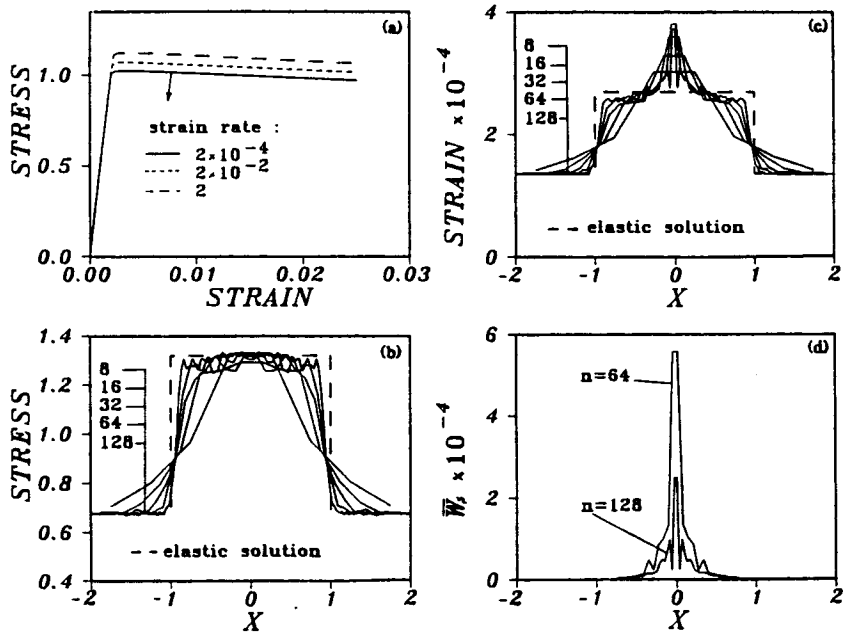

Figure 4 (a) Rate-dependent model; convergence of the stress (b), strain (c), and softening energy distribution (d) with mesh refinement

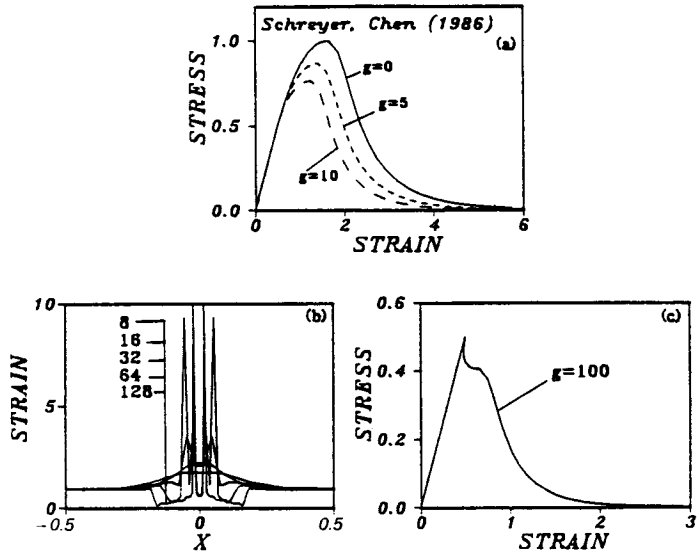

Figure 5 (a) Schreyer and Chen's non-local model; convergence of the strain profiles (b), influence of a high strain gradient on the stress–strain response (c)

monotonic loading, their constitutive relations are:

$$\text{for } 0 \leqslant \varepsilon^p \leqslant \varepsilon_L^p: \quad \sigma = H_0 + (H_L - H_0)\sin\left[\frac{\pi}{2}\left(\frac{\varepsilon^p}{\varepsilon_L^p}\right)^n\right]$$

$$\text{for } \varepsilon^p > \varepsilon_L^p: \quad \sigma = H_a + (H_L - H_a)(1 + a_1\varepsilon^*)\exp(-a_1\varepsilon^*) \tag{22}$$

where ε^p is the inelastic strain, ε_L^p is the value of the strain at the peak stress and ε^* is the relative plastic strain:

$$\varepsilon^* = \frac{\varepsilon^p - \varepsilon_L^p}{\varepsilon_L^p} \tag{23}$$

H_0 is interpreted as the initial yield stress, H_a as the residual stress ($\varepsilon \to \infty$), and H_L as the peak stress. The plastic strain gradient $\varepsilon_{,x}^p$ affects the peak stress and the softening parameters:

$$H_L = H_{lo}G, \quad \varepsilon_L^p = \varepsilon_{lo}^p G, \quad G = a_2 + (1 - a_2)\exp(-a_3|\varepsilon_{,x}^p|) \tag{25}$$

H_{lo} and ε_{lo}^p are constants corresponding to $\varepsilon_{,x}^p = 0$; a_2, a_3 are material constants. At unloading, the stress–strain relation is linear elastic, E is Young's modulus.

Figure 5a shows the influence of the strain gradient on the stress–strain curve. The same material parameters as indicated in Reference 22 are chosen: $H_0 = 0.5$, $H_{lo} = 1$, $\varepsilon_{lo}^p = 0.6$, $E = 1$, $H_a = 0$, $n = 0.5$, $a_1 = 0.8$, $a_2 = 0.4$, $a_3 = 0.05$. As G increases, the peak stress, the peak strain and the softening energy $\bar{W}_f$ decrease. The softening portion of the curve becomes sharper. The wave propagation analysis is carried out with $\rho = 1$, $c = 0.825$ and $\Delta t = 5 \times 10^{-3}$.

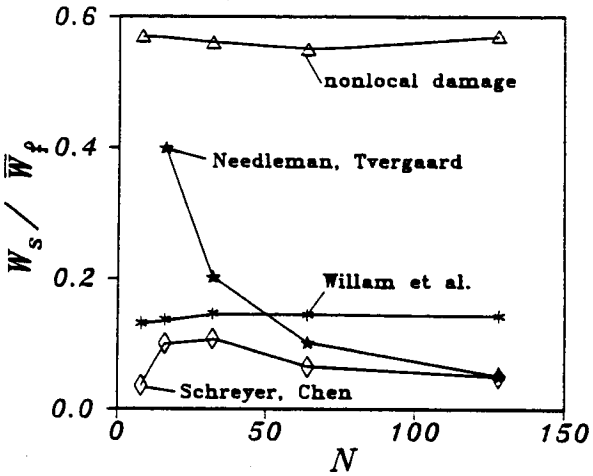

Figure 6 Convergence of the energy dissipated by softening as a function of the number of finite elements of constant length

From *Figure 5b* and the convergence of the energy dissipated by softening in *Figure 6*, we may notice that the results are less convincing than the static localization analysis[22]. In fact, the strain profiles are not very different from the usual continuum calculations. Once localization occurs, the strain at the middle of the bar remains finite but very large strains are encountered in the adjacent elements. This may be attributed to the type of response in which the strain gradient $\varepsilon^p_{,x}$ at the wave front becomes very high. In this case *Figure 5c* shows that the stress–strain curve exhibits snapback. Such a result should be rejected, since this instability should be a structural characteristic rather than a material property. This spurious response is obtained when the influence of the gradient becomes predominant and the strains are negligible compared to $\varepsilon^p_{,x}$.

It may be more appropriate to consider the second spatial derivatives. Triantafyllidis and Aifantis[23] used the second derivative of strain in a constitutive law of the form:

$$\sigma = f(\hat{\varepsilon}), \qquad \hat{\varepsilon} = \varepsilon + \alpha \varepsilon_{,xx} \tag{25}$$

The strain $\hat{\varepsilon}$ in (25) may be obtained by Taylor series expansion of the non-local strain $\bar{\varepsilon}$:

$$\bar{\varepsilon} = \frac{1}{l} \int_{-l/2}^{l/2} \varepsilon(x+s)\, \mathrm{d}s \tag{26}$$

in which l is called the characteristic length. In this case the coefficient α in (25) is $l^2/24$[21,24].

Bažant[24], and Lasry and Belytschko[21] used similar relations. Satisfactory results have been obtained with non-zero energy dissipated at failure, W_s, finite-size localization zones[21] and non-zero finite specific energy $\bar{W}_f$. However, this type of localization limiter presents a major drawback: with an equation of the type of (25), the solution of equilibrium states requires an additional boundary condition which involves $u_{,xx}$ (i.e. the second derivative of displacement) whose physical meaning remains to be clarified. Since the equations of equilibrium are of a higher order, additional boundary conditions are needed and higher-order finite elements are required in numerical analysis.

Replacing $\hat{\varepsilon}$ by $\bar{\varepsilon}$ in the constitutive law gives a limiter of the second type. This averaging method, which was inspired by the classical non-local theories of elasticity[33] and was successfully used by Bažant *et al.*[34], requires imbrication (overlapping) of finite elements. This is a drawback of this method in numerical implementation. Called the imbricate continuum, this method may be regarded as a counterpart of higher-order finite elements where averages are calculated by means of a mesh of imbricated elements. The equations of equilibrium are again non-standard. We may note that no additional boundary conditions are required in the imbricated finite element system, although the type of averaging is different at the boundary of the solid. This last consequence of averaging-type localization limiters seems more realistic even if the choice of the averaging method near the boundaries, where the averaging domain of size l protrudes outside the body, has not been physically justified.

In the latest work[28,35,36] a modified version of the averaging type of localization limiter was proposed. Called the non-local continuum with local strain, this formulation applies non-local averaging only to those variables that control strain-softening. Such non-local parameters may be the fracturing strain or damage[28], or the yield limit[36]. In the scalar damage model, the constitutive law is:

$$\sigma = (1-\Omega) E \varepsilon \tag{27}$$

where Ω is the non-local damage defined as:

$$\Omega = f(\bar{Y}), \qquad \bar{Y} = \frac{1}{l} \int_{-l/2}^{l/2} Y(x+s)\, \mathrm{d}s \tag{28}$$

E is the initial Young's modulus of the material and l is the characteristic length, a material parameter. The non-local damage is a function of the mean energy release rate $\bar{Y}$ calculated by averaging the local damage energy release rate Y over a domain of length l[28]:

$$Y(x) = \tfrac{1}{2} E \varepsilon^2(x) \tag{29}$$

This localization limiter gives satisfactory results for wave propagation analysis as well as static strain localization[28,36]. As exemplified in *Figure 6*, a good convergence of the dynamic calculations is achieved in terms of energy. This calculation also yields a constant size h of the localization zone ($h \approx 1.88l$).

There exist also some physical arguments for this type of localization limiter. Non-local elasticity has originally been introduced to extend the applicability of elastic continuum theories to atomic lattices[33]. Its purpose is to approximate the large scale behaviour of a material that cannot be regarded as a continuum microscopically. Therefore, the strain can no longer be defined in the continuum sense, and a modified strain definition of the type of (26) is required, such that $\varepsilon \approx \bar{\varepsilon}$ if the material is viewed at the macroscopic level. A transition between the continuum and the lattice descriptions is achieved by this formulation in which the non-local part becomes more important (with respect to ε) as the characteristic length of the material becomes non-negligible. Non-local theories of elasticity may be viewed as methods to calculate the response of materials in the range where the characteristic length cannot be neglected, compared to the size of the structure.

Strain-softening is a phenomenon that lies at the next larger scale. It consists of material-structure interaction. Prior to localization, damage is distributed in the structure. Later the damage zone evolves into a

macrocrack as localization becomes sharp. This progressive transition can be described neither by continuum nor fracture type theories. We chose to extend the applicability of the continuum method by modifying the parameter that is producing the strain-softening response: the damage in the present example. Localization into a line crack is not admissible in a continuum damage solution since it violates the definition of damage itself. This variable should remain distributed such that the material may be regarded as a continuum. We have shown that, with continuum models, the size of the localization zone is much smaller than the characteristic length (in the statistical sense) and damage becomes discontinuous.

Similarly to (26), we may redefine the damage variable ω called in this case the non-local damage, Ω. By definition, Ω is continuous. As demonstrated[36], the size of the localization zone is proportional to the characteristic length l. Under this condition the fracture mechanics solution is reached in the limit of an infinite structure size compared to l.

The transition from a material model to a structure type of model may be simplified in one dimension to the interaction between the localization zone and the rest of the solid. We analyse the uniaxial response of several bars of different lengths. The non-local damage model is used with a damage evolution law similar to that in Reference 28:

$$\text{If } F(\bar{Y})=0 \text{ and } \dot{F}(\bar{Y})=0 \quad \text{then}$$

$$\Omega=1-(1+b_1(Y-Y_1)+b_2(Y-Y_1)^2)^{-1} \quad (30)$$

$$\text{If } F(\bar{Y})=0 \text{ and } \dot{F}(\bar{Y})<0 \text{ or if } F(\bar{Y})<0 \quad \text{then}$$

$$\dot{\Omega}=0 \quad (31)$$

where $F(\bar{Y})=\bar{Y}-\kappa(\bar{Y})$. F is the loading function of damage, κ is the softening parameter, representing the maximum value of $\bar{Y}$ ever reached at the considered point, and the initial value of κ is Y_1. In numerical computations we take $b_1=20$, $b_2=0.5$, $Y_1=8540\times10^{-6}$, and $E=32{,}000$ MPa. Four different lengths L of specimen are considered: $L/l=1, 2, 4, 8$ while the cross-section is kept constant. We use finite bar elements of constant length $L_e=l/5$. To initiate localization at the middle of the bar, the element at the centre of the bar is considered to be weaker, its damage threshold Y_1 reduced by 1% compared to the other elements. The secant, direct iteration method is chosen.

Figure 7a shows the calculated responses in terms of the stress and the mean strain (defined as the relative displacement divided by the total length). Because of localization, the response is not unique; a very significant size effect is found. For $L/l=1$ the material stress–strain diagram is recovered, while for large L/l a sharp post-peak sharp drop to zero stress is obtained, similar to unstable crack propagation. As expected, the non-local damage model gives all the transitory states in which the resulting descent of the post-peak stress–displacement diagram becomes steeper as the size of the bar grows compared to the localization zone size (or characteristic length). The end segment of the plot of the post-peak displacement *versus* stress in *Figure 7b* shows that the curve could almost be considered as a unique characteristic of the material once localization has occurred. In this range, the results are similar to the experimental measurement on which the fracture-type

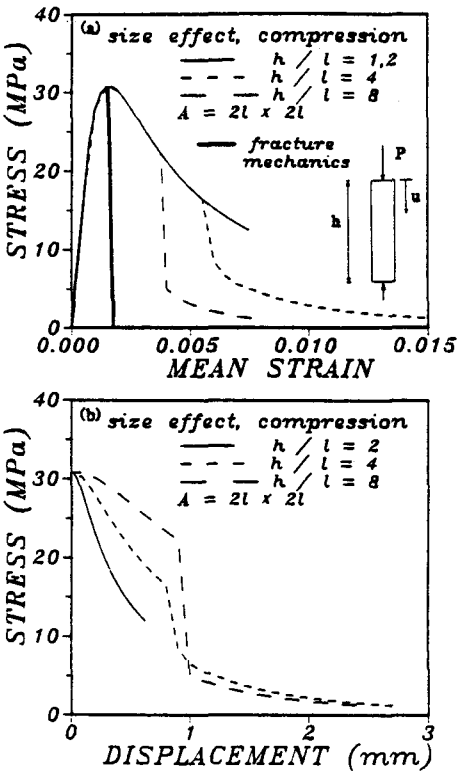

Figure 7 Size effect in compression: stress *versus* mean strain and stress *versus* post-peak displacement curves (b, c)

models were based[14,15]. The energy dissipated through softening, W_s (i.e. the area under the curve in *Figure 7b*) is finite.

DIFFERENTIAL APPROXIMATION OF NON-LOCAL DAMAGE

The differential approximation of the non-local damage model may be developed as follows. We consider the constitutive law, (27), and define the non-local damage as:

$$\Omega=\frac{1}{l}\int_{-l/2}^{l/2}\omega(x+s)\,ds \quad (32)$$

where ω is the local damage. Assuming the characteristic length l to be small compared to the structure size, and ω to change little over length l, we may expand ω in Taylor series:

$$\omega(x+s)=\omega(x)+\omega'(x)s+\tfrac{1}{2}\omega''(x)s^2+O(s^2) \quad (33)$$

$\omega'(x)$ and $\omega''(x)$ are the derivatives of damage with respect to x. Substituting (33) into (32) gives:

$$\Omega(x)\approx\omega(x)+\frac{l^2}{24}\omega''(x) \quad \text{(interior points)} \quad (34)$$

provided the averaging domain does not protrude beyond the boundary. For a point at the boundary, the averaging can be made only between $s=0$ and $s=l/2$, so that:

$$\Omega(x)\approx\omega(x)+\frac{l}{4}\omega'(x) \quad (35)$$

Similar differential approximations apply to other averages, e.g. those of strain, stress, strength or yield

limit. In view of (34) and (35), the formulations using the first gradient of strain or the first gradient of strength appear to be appropriate only when failure is dominated by damage near the boundaries (as in bending), while those using the second gradient appear to be appropriate only when failure is dominated by damage at the interior (e.g., when failure develops from an interior crack).

For numerical calculations the second and first derivatives may be approximated by finite differences:

$$\omega_k'' = \frac{\omega_{k+1} - 2\omega_k + \omega_{k-1}}{L_e^2}, \qquad \omega_k' = \frac{\omega_j - \omega_i}{L_e} \quad (36)$$

subscript k refers to the element number, subscripts i and j refer to the nodes of the element, and L_e = length of the finite elements = constant. *Figure 8* shows the non-local damage profiles obtained for our simple wave propagation problem. Convergence towards a solution in which a region of finite size is completely damaged is observed as the mesh is refined. Numerical difficulties similar to those reported earlier[21] were encountered since the damage profile is discontinuous at the boundary of the damage region. Calculation of the damage derivatives could not be properly carried out for a mesh of very small elements.

The damage profiles in *Figure 8* suggest that Ω is discontinuous at the interface between the localization zone and the unloading part of the bar. At this point the Taylor series expansion in (33) is not valid. The differential approximation yields results that are inconsistent with our assumption, as could have been expected. The equations of equilibrium that are approximated by the finite element solution are standard. Therefore the strain is a C_0 function, and Ω is also a C_0 function. It is not required that the second derivative of strain be defined. We can remark that this would not happen in the fully non-local solution[37], since higher-order differential equations are solved and continuity of a higher-order is required.

Furthermore, we may look at the continuity of the non-local damage at the boundary of the localization zone. From the solution in Reference 36, the first derivative of Ω inside the localization zone is approximated as:

$$\Omega'(x) = \frac{1}{l}\left[\omega\left(x + \frac{l}{2}\right) - \omega\left(x - \frac{l}{2}\right)\right] \quad (37)$$

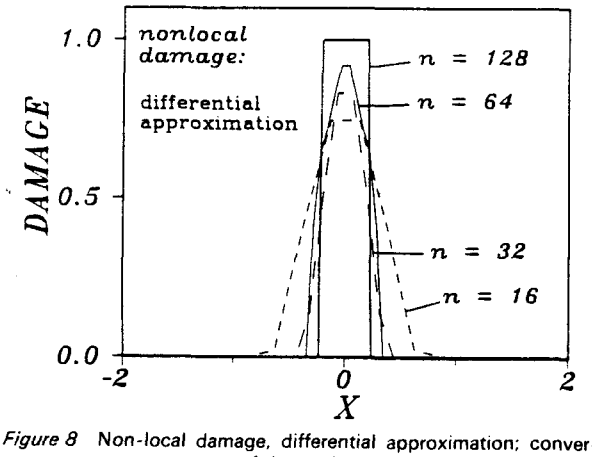

Figure 8 Non-local damage, differential approximation; convergence of the strain profiles

and outside we have $\Omega' = 0$ since the initial state of damage is $\Omega = 0$. The analytical solution[36] shows that Ω' and ω are not continuous across the boundary of the localization zone but they jump from zero to a finite value. The expansion in (33) is not even comparable with the analytical solution obtained from the non-local damage theory. The differential approximation cannot be used in this type of continuum. However, it may be applied in the fully non-local solution where higher-order differential equations yield a continuity condition in accordance with a Taylor series expansion of the strain.

CONCLUSIONS

1. A non-zero size of the strain-localization zone cannot be achieved by either the continuum or fracture mechanics models. Both formulations yield results in which the strain-softening zone cannot propagate, in agreement with Hadamard instability.

2. In the fracture mechanics models, the energy ultimately dissipated by the structure due to strain softening is constant. However, this is achieved because failure is reached instantaneously in an infinitesimal volume of material whose behaviour is nearly elastic-perfectly plastic and the specific failure energy (per unit volume) tends to infinity. The strain at the localization point is infinite. As shown by the analytical solutions of wave propagation, the response of this type of model is very close to the response of elastic perfectly plastic models which exhibits no strain softening.

3. Despite the fact that rate dependence prevents the partial differential equation of motion from becoming elliptic and ensures that the problem is well posed, the results are not quite satisfactory. At localization the strains are finite but the localization zone tends to an infinitely small size. Similar to continuum rate-independent models in which softening is caused by void growth in a non-softening homogeneous matrix, the energy dissipated at failure is found to converge to zero in these rate-dependent models.

4. Solving strain-softening problems with a continuum-type material model requires the use of localization limiters which may be put into two categories. The first involves the use of higher-order spatial derivatives of displacements in the constitutive law, while the second involves some non-local concept based on spatial averaging to achieve a realistic description of the strain-localization instability.

5. The use of higher-order derivatives implies the equations of motion to be high-order differential equations. Additional boundary conditions, whose physical meaning needs to be clarified, are required. This type of localization limiter may be viewed as a special case of the non-local models if the averaged variable is expanded in Taylor series.

6. A simple limiter of the averaging kind is the non-local continuum with local strain, whose salient characteristic is that the energy dissipation is non-local but the strain (and especially the elastic response) is local. Applied to 1-D static and dynamic problems and 2-D numerical computations, this method was proved to be computationally very effective and easy to program. The non-local continuum with local strain may serve as a convenient model to handle the transition between the problems in which the damage zone is large compared to the characteristic length of the continuum and the

problems in which the damage zone is so localized that it can be viewed as a line crack. The significant size effect due to the strain-softening portion of the uniaxial response is adequately modelled by this model. The results generally agree with experimental evidence.

7. The use of higher-order derivatives may be regarded as an approximation to the non-local averaging rule. In this light, the use of first spatial derivatives (gradients) of damage, strain or strength appears appropriate only when failure is dominated by damage near the boundaries, while the use of second spatial derivatives is appropriate when damage in the interior dominates. However, the differential approximation cannot be properly used for the non-local continuum with local strain. When localization develops, the assumptions underlying the Taylor expansion of the non-local damage cannot be met since continuity of the local damage is not required.

ACKNOWLEDGMENTS

Financial support under US Air Force of Scientific Research contract No. F49620-87-C-0030DEF with Northwestern University, monitored by Dr. Spencer T. Wu, is gratefully acknowledged. Thanks are due to Nadine Pijaudier-Cabot for her expert secretarial services.

REFERENCES

1 Bažant, Z. P. Mechanics of distributed cracking, *Appl. Mech. Rev.*, **39**, 675–705 (1985)
2 Krajcinovic, D. Constitutive equations for damaging materials, *J. App. Mech.*, **50**, 355–360 (1983)
3 Mazars, J. and Pijaudier-Cabot, G. Continuum damage theory: application to concrete, *Int. Report No. 71*, Laboratoire de Mécanique et Technologie, ENS de Cachan, France (1986); *J. Eng. Mech., ASCE*, in press
4 Gurson, A. L. Continuum theory of ductile rupture by void nucleation and growth: Part I—Yield criteria and flow rules for ductile media, *J. Eng. Mat. Tech.*, **99**, 2–15 (1977)
5 Needleman, A. and Tvergaard, V. An analysis of ductile rupture in notched bars, *J. Mech. Phys. Solids*, **3**, 461–490 (1984)
6 De Borst, R. and Nauta, P. Non-orthogonal cracks in a smeared finite element model, *Eng. Comput.*, **2**, 35–46 (1985)
7 Pietruszczak, S. and Mróz, Z. Finite element analysis of deformation of strain-softening materials, *Int. J. Num. Meth. Eng.*, **17**, 327–334 (1981)
8 Needleman, A. Material rate dependence and mesh sensitivity in localization problems, *Comp. Methods Appl. Mech. Eng.*, **67**, 69–85 (1988)
9 Sandler, I. S. Strain-softening for static and dynamic problems, in *Proc. Symp. Constit. Equations: Micro, Macro and Computational Aspects. ASME, Winter Annual Meeting, New Orleans* (Ed. K. J. Willam), ASME, New York, pp. 217–231 (1984)
10 Bažant, Z. P. Instability, ductility and size effect in strain-softening concrete, *J. Eng. Mech. Div., ASCE*, **102**, (EM2), 331–344 (1976); *Discuss.*, **103**, 357–358, 775–777; **104**, 501–502
11 Bažant, Z. P. and Belytschko, T. B. Strain-softening continuum damage: localization and size effect, in *Int. Conf. Constit. Laws Engin. Mat., Tucson*, Vol. 1 (Ed. C. S. Desai *et al.*), Elsevier, New York, pp. 11–33 (1987)
12 Hillerborg, A., Modeer, M. and Petersson, P. E. Analysis of crack formation and crack growth in concrete by means of fracture mechanics and finite elements, *Cement Concr. Res.*, **6**, 773–782 (1976)
13 Ingraffea, A. and Saouma, V. *Numerical Modeling of Discrete Local Propagation in Reinforced and Plain Concrete* (Ed. G. C. Sih and A. DiTommaso), Martinus Nijhoff, The Hague, pp. 171–225 (1984)
14 Willam, K. J., Bicanic, N. and Sture, S. Experimental, constitutive and computational aspects of concrete failure, *US–Japan Semin. Finite Element Analysis of Reinforced Concrete*, pp. 149–172 (1985)
15 Willam, K., Bicanic, N., Pramono, E. and Sture, S. Composite fracture model for strain-softening computations of concrete, in *Fracture Toughness and Fracture Energy of Concrete* (Ed. F. H. Wittmann), Elsevier, New York, pp. 149–162 (1986)
16 Van Mier, J. G. M. Multiaxial strain-softening of concrete, Parts 1 & 2, *Mat. Construct.*, **19**, 179–200 (1986)
17 Joseph, D., Renardy, M. and Saut, J. C. Hyperbolicity and change of type in the flow of viscoelastic fluids, *Arch. Rational Mech. Anal.*, **87**, 213–251 (1985)
18 Donea, J. A Taylor–Galerkin method for convective transport problems, *Int. J. Num. Meth. Eng.*, **20**, 101–119 (1984)
19 Hughes, T. J. R. and Brooks, A. N. A theoretical framework for Petrov/Galerkin methods with discontinuous weighting functions: application to the stream line upwind procedure, in *Finite Element in Fluids* (Ed. R. H. Gallagher), J. Wiley, Chichester, Vol. 4, pp. 47–65 (1982)
20 Richtmeyer, R. D. and Morton, K. W. *Difference Methods for Initial-Value Problems*, Interscience, New York, 2nd Edn (1967)
21 Lasry, D. and Belytschko, T. Gradient-type localization limiters for strain-softening problems, *Report*, Northwestern University, Evanston, IL (1987)
22 Schreyer, H. L. and Chen, Z. One dimensional softening with localization, *J. Appl. Mech.*, **53**, 791–797 (1986)
23 Triantafyllidis, N. and Aifantis, E. A gradient approach to localization of deformation. I. Hyperelastic materials, *J. Elasticity*, **16**, 225–237 (1986)
24 Bažant, Z. P. Imbricate continuum and its variational derivation, *J. Eng. Mech. Div., ASCE*, **110**, 1693–1712 (1984)
25 Bažant, Z. P. and Belytschko, T. B. Wave propagation in a strain-softening bar: exact solution, *J. Eng. Mech. Div., ASCE*, **111**, 381–389 (1985)
26 Legendre, D. Prévision de la ruine des structures en béton par une approche combinée: mécanique de l'endommagement/mécanique de la rupture, *Thèse de 3ème Cycle*, Université Paris VI (1985)
27 Ottosen, N. S. Thermodynamic consequences of strain-softening in tension, *J. Eng. Mech. Div., ASCE*, **112**, 1152–1164 (1986)
28 Pijaudier-Cabot, G. and Bažant, Z. P. Nonlocal damage theory, *J. Eng. Mech. Div., ASCE*, **113**, 1512–1533 (1987)
29 Read, H. E. and Hegemier, G. P. Strain-softening of rock, soil and concrete—a review article, *Mech. Mat.*, **3**, 271–294 (1984)
30 Wu, F. H. and Freund, L. B. Deformation trapping due to thermoplastic instability in one-dimensional wave propagation, *J. Mech. Phys. Solids*, **32**, No. 2, 119–132 (1984)
31 Floegl, H. and Mang, H. A. On tension-stiffening in cracked reinforced concrete slabs and shells considering geometic and physical nonlinearity, *Ing. Archiv*, **51**, 215–242 (1981)
32 Mang, H. and Eberhardsteiner, J. Collapse analysis of thin R.C. shells on the basis of a new fracture criterion, *US–Japan Semin. Finite Element Analysis of Reinforced Concrete Structures*, pp. 217–238 (1985)
33 Eringen, A. C. Linear theory of nonlocal elasticity and dispersion of plane waves, *Int. J. Eng. Sci.*, **10**, 425–435 (1972)
34 Bažant, Z. P., Belytschko, T. B. and Chang, T. P. Continuum theory for strain-softening, *J. Eng. Mech. Div., ASCE*, **110**, 1666–1692 (1984)
35 Bažant, Z. P., Lin, F. B. and Pijaudier-Cabot, G. Yield limit degradation: nonlocal continuum with local strains, in *Int. Conf. Comput. Plast., Barcelona* (Ed. E. Oñate, R. Owen and E. Hinton), University of Wales, Swansea, pp. 1757–1779 (1987)
36 Bažant, Z. P. and Pijaudier-Cabot, G. Nonlocal damage: continuum model and localization instability, *Report No. 87-2/428n-1*, Center of Concrete and Geomaterials, Northwestern University, Evanston, IL (1987); Nonlocal continuum damage, localization instability and convergence, *J. Appl. Mech., ASME*, in press
37 Bažant, Z. P. and Zubelewicz, A. Strain-softening bar and beam; exact nonlocal solution, *Report No. 86-12-428s*, Center for Concrete and Geomaterials, Northwestern University, Evanston, IL (1986); *Int. J. Solids Struct.*, in press